Dalton Transactions

ARTICLE

Stannylenes based on pyrrole-phosphane and dipyrromethane-diphosphane scaffolds: Syntheses and behavior as precursors to PSnP pincer palladium(II), palladium(0) and gold(I) complexes †

Received 00th September 2021,
Accepted 00th September 2021

DOI: 10.1039/x0xx00000x

www.rsc.org/

Javier A. Cabeza,[a]* Israel Fernández,[b] Pablo García-Álvarez,[a] Rubén García-Soriano,[a] Carlos J. Laglera-Gándara[a] and Rubén Toral[a]

2-Ditertbutylphosphanylmethylpyrrole (H_2pyrmP^{t}Bu$_2$) and 2,2'-bis(diisopropylphosphanylmethyl)-5,5'-dimethyldipyrromethane ((HpyrmP^{i}Pr$_2$)$_2$CMe$_2$) have been used to synthesize new P-donor-stabilized stannylenes in which the Sn atom is attached to one, SnCl(HpyrmP^{t}Bu$_2$) (**1**) and Sn{N(SiMe$_3$)$_2$}(HpyrmP^{t}Bu$_2$) (**2**), or two pyrrolyl-phosphane scaffolds, Sn(HpyrmP^{t}Bu$_2$)$_2$ (**3**), or to a dipyrromethane-diphosphane scaffold, Sn(pyrmP^{i}Pr$_2$)$_2$CMe$_2$ (**4**). It has been found that stannylenes **3** and **4** are excellent precursors to transition metal complexes containing PSnP pincer-type ligands. Their reactions with chlorido transition metal complexes have afforded [PdCl{κ^3*P*,*Sn*,*P*-SnCl(HpyrmP^{t}Bu$_2$)$_2$}] (**6**) [PdCl{κ^3*P*,*Sn*,*P*-SnCl(pyrmP^{i}Pr$_2$)$_2$CMe$_2$}] (**7**) and [Au{κ^3*P*,*Sn*,*P*-SnCl(HpyrmP^{t}Bu$_2$)$_2$}] (**8**), which contain a PSnP pincer-type chloridostannyl ligand. While complexes **6** and **7** are square-planar palladium(II) complexes, compound **8** is an uncommon gold(I) complex having a T-shaped coordination geometry with a very long Sn–Au bond (3.120 Å). The T-shaped palladium(0) complex [Pd{κ^3*P*,*Sn*,*P*-Sn(pyrmP^{i}Pr$_2$)$_2$CMe$_2$}] (**9**), which contains an unprecedented PSnP pincer-type stannylene that behaves as a *Z*-type (σ-acceptor) ligand, has been prepared from **4** and [Pd(η^3-C$_3$H$_5$)(η^5-C$_5$H$_5$)].

Introduction

The search for new pincer ligands is currently a very active research topic because the balance between reactivity and stability often provided by these ligands to their metal complexes has been recognized as of utmost relevance to the excellent catalytic applications that have been found for many of these complexes.[1,2] As catalytically efficient metal complexes frequently require strong electron-donating groups, many pincer ligands having an N-heterocyclic carbene (NHC) as the central C-donor group have already been reported.[3] However, although heavier carbene analogues (silylenes, germylenes and stannylenes) can also be very strong electron-donating groups[4] and some of their metal complexes have already demonstrated excellent catalytic activities,[5,6] their participation in pincer complexes is still limited to very few ECE,[6j-l,7] ENE,[6d,6h,6i,6n] and PEP [8–16] systems (E = Si, Ge or Sn).

In the context of metal-free PEP heavier tetrylenes (E = Ge, Sn; silylenes of this type are yet unknown) that can be precursors to pincer complexes,[17] we reported the first PGeP germylene in 2017, Ge(NCH$_2$P^{t}Bu$_2$)$_2$C$_6$H$_4$,[10] and managed to prepare some transition metal complexes with it,[10,18] but the short length of its CH$_2$P^{t}Bu$_2$ sidearms and the particular geometry of its benzogermole core resulted in very distorted coordination geometries. Looking for more appropriate ligand frameworks, we have recently prepared the pyrrole-based PGeP germylenes Ge(HpyrmP^{t}Bu$_2$)$_2$[12] (HpyrmP^{t}Bu$_2$ = 2-ditertbutylphosphanylmethylpyrrole) and Ge(pyrmP^{i}Pr$_2$)$_2$CMe$_2$[13] ((pyrmP^{i}Pr$_2$)$_2$CMe$_2$ = 2,2'-bis(diisopropylphosphanylmethyl)-5,5'-dimethyldipyrromethane) and have shown that their PGeP pincer transition metal complexes do not present distorted coordination geometries.[12,13,19]

Regarding PSnP stannylenes that can be precursors to pincer ligands, only four specimens of this family have so far been reported (Figure 1), namely, Sn(NCH$_2$P^{t}Bu$_2$)$_2$C$_6$H$_4$ (**A**),[16] Sn(NC$_6$H$_4$PPh$_2$)$_2$C$_2$H$_4$ (**B**),[11] and SnX(NC$_6$H$_4$PPh$_2$)$_2$C$_3$HMe$_2$ (**C**; X = Cl, PCO),[15] but stannylene **A** has as yet failed to render PSnP pincer complexes (it has only behaved as a bidentate SnP-chelating ligand),[16] only one complex has so far been identified as derived from stannylene **B**, that is the platinum(0) PSnP pincer complex [Pt{κ^3*P*,*Sn*,*P*-Sn(NC$_6$H$_4$PPh$_2$)$_2$C$_2$H$_4$}],[11] and no transition metal derivative has yet been prepared from stannylenes of type **C**.[15] Therefore, this research field is still at a very early stage of its development.

[a]*Centro de Innovación en Química Avanzada (ORFEO-CINQA), Departamento de Química Orgánica e Inorgánica, Universidad de Oviedo, 33071 Oviedo, Spain.*
[b]*Centro de Innovación en Química Avanzada (ORFEO-CINQA), Departamento de Química Orgánica I, Facultad de Ciencias Químicas, Universidad Complutense de Madrid, 28040 Madrid, Spain.*
*E-mail: jac@uniovi.es (J.A.C.).
†Electronic Supplementary Information (ESI) available: CCDC 2097501–2097505. NMR spectra and complementary XRD and DFT data. See DOI: 10.1039/x0xx00000x.

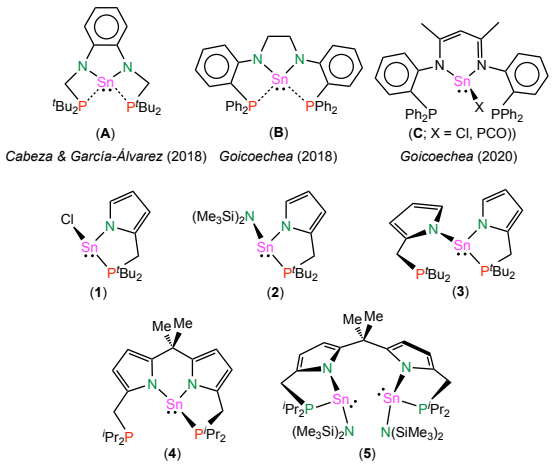

Fig. 1 The previously known stannylenes that can lead to PSnP pincer complexes (**A**–**C**) and the stannylenes reported in this work (**1**–**5**).

As easily available transition metal complexes containing PSnP pincer ligands are desirable (they are expected to display novel structural, bonding and catalytic properties), we targeted the synthesis of the tin analogues of the PGeP germylenes Ge(HpyrmP^{t}Bu$_2$)$_2$ and Ge(pyrmP^{i}Pr$_2$)$_2$CMe$_2$ (compounds **3** and **4** in Fig. 1) because, as mentioned above, these germylenes have already allowed the synthesis of a variety of PGeP pincer transition metal complexes.

We now report the successful preparation of the PSnP stannylenes **3** and **4** (in addition to stannylenes **1**, **2**, and **5**; Fig. 1) and their reactions with selected transition metal complex precursors. These reactions have rendered complexes containing PSnP pincer-type chloridostannyl ligands (compounds **6**–**8**) and a complex in which its PSnP pincer ligand is a stannylene (compound **9**). Compounds **8** and **9** also display some additional features of interest because both have a T-shaped metal coordination geometry that is infrequent for gold(I) (**8**) and palladium(0) (**9**) and, additionally, the stannylene fragment of **9** behaves as a *Z*-type (σ-acceptor) ligand, a yet uncommon coordination mode for stannylenes.

Results and discussion

Two alternative synthetic methods were satisfactorily used to prepare the PSnP stannylene Sn(HpyrmP^{t}Bu$_2$)$_2$ (**3**; Scheme 1). Deprotonation of 2-ditertbutylmethylpyrrole (H$_2$pyrmP^{t}Bu$_2$)[12] with BuLi and treatment of the resulting lithiated species with SnCl$_2$ in 2:1 mole ratio allowed the isolation of **3** in 67% yield. A greater yield, 94%, was achieved by treating H$_2$pyrmP^{t}Bu$_2$ with Sn{N(SiMe$_3$)$_2$}$_2$ in 2:1 mole ratio. The intermediate monophosphane stannylenes SnCl(HpyrmP^{t}Bu$_2$) (**1**) and Sn{N(SiMe$_3$)$_2$}(HpyrmP^{t}Bu$_2$) (**2**) were also prepared from similar reactions but using a 1:1 mole ratio of the phosphane and tin reagents (Scheme 1). The related pyrrolyl-amino stannylenes Sn{N(SiMe$_3$)$_2$}(HpyrmNMe$_2$) and Sn(HpyrmNMe$_2$)$_2$ have been previously prepared from H$_2$pyrmNMe$_2$ and Sn{N(SiMe$_3$)$_2$}$_2$.[20]

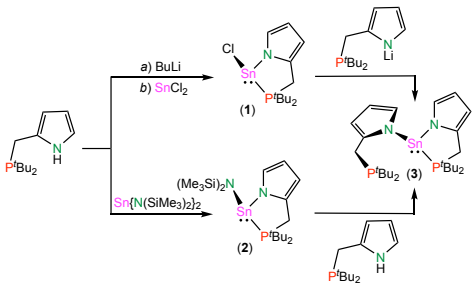

Scheme 1 Alternative syntheses of stannylene **3**.

The dipyrromethane-derived PSnP stannylene Sn(pyrmP^{i}Pr$_2$)$_2$CMe$_2$ (**4**) could not be satisfactorily prepared by treating SnCl$_2$ with dilithiated 2,9-bis(diisopropylphosphanylmethyl)-5,5-dimethyldipyrromethane. Nevertheless, **4** could be isolated in 34% yield by treating (HpyrmP^{i}Pr$_2$)$_2$CMe$_2$[13] with Sn{N(SiMe$_3$)$_2$}$_2$ in 1:1 mole ratio (Scheme 2). The use of larger amounts of Sn{N(SiMe$_3$)$_2$}$_2$ favored the formation of distannylene Sn$_2${N(SiMe$_3$)$_2$}$_2${(pyrmP^{i}Pr$_2$)$_2$CMe$_2$} (**5**) (Scheme 2), but this compound could not be satisfactorily separated from stannylene **4** and Sn{N(SiMe$_3$)$_2$}$_2$. In fact, we subsequently confirmed by ^{31}P{^{1}H} NMR that, in solution, compounds **5**, **4** and Sn{N(SiMe$_3$)$_2$}$_2$ coexist in equilibrium. A few crystals of **5** suitable for XRD were obtained by keeping at –18 °C a hexane solution containing a 4:1:5 molar mixture of **5**, **4** and Sn{N(SiMe$_3$)$_2$}$_2$.

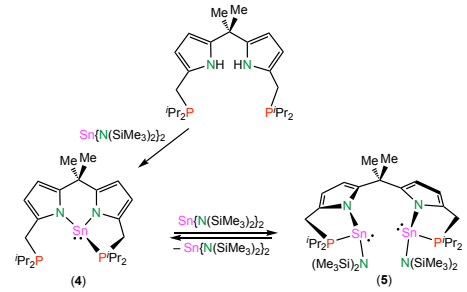

Scheme 2 Synthesis of stannylenes **4** and **5**.

The solid-state X-ray diffraction (XRD) structures of **3** (Fig. 2) and **4** (Fig. 3) showed that these compounds are donor-stabilized stannylenes, with the Sn atom attached to the two pyrrolyl N atoms and with one of their two phosphane fragments acting as the donor group, Sn1–P1 2.7194(4) Å in **3** and 2.7378(5) Å in **4**. Curiously, in both compounds, the Sn atom is not far away from the P atom of the pendant phosphane side-arm, Sn1···P2 3.5554(6) Å in **3** and 3.7626(7) Å in **4**, suggesting the existence of some interaction between these atoms. These Sn–P distances contrast with those found in the previously-known PSnP stannylenes **A** and **B** (Figure 1), which are very similar within each compound, 3.277(1) and 3.313(1) Å in **A**[16] and 2.839(1) and 2.762(1) Å in **B**[11] (the rigid imidazole-type core of **A** and the short length of its phosphane side-arms do not allow a shorter approach of the P atoms to the Sn atom). While the planes defined by the pyrrole rings of **3** are almost perpendicular to each other (dihedral angle = 97.86(5)°), those of **4** form a dihedral angle of 140.57(8)°. These molecular structures are reminiscent of those of their germanium

analogues,[12,13] but the larger size of tin provokes the E–N and E–P bond distances to be notably longer (*ca.* 0.2 Å) for E = Sn than for E = Ge. Curiously, it has been reported that stannylene $Sn(HpyrmNMe_2)_2$, which is related to **3** but has NMe_2 instead of P^tBu_2 groups, presents equal Sn–NMe_2 distances (2.52 Å) and a seesaw molecular structure (trigonal bipyramidal coordination geometry with the tin lone pair and the pyrrolyl N atoms in the equatorial positions).[20] Therefore, the large difference found between the Sn–P distances of stannylene **3** may have a steric origin, associated with the large steric bulk of the P^tBu_2 groups. However, the rigidity imposed by the dipyrromethane core of **4** impedes a trigonal bipyramidal coordination geometry of the Sn atom analogous to that of $Sn(HpyrmNMe_2)_2$.

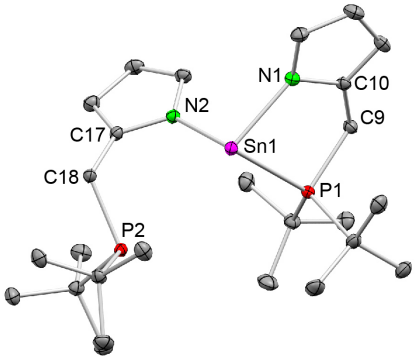

Fig. 2 XRD molecular structure of **3** (40% displacement ellipsoids, H atoms have been omitted for clarity). Selected bond lengths (Å) and angles (°): Sn1–N1 2.180(1), Sn1–N2 2.128(1), Sn1–P1 2.7194(4), Sn1···P2 3.5554(6); N1–Sn1–N2 93.68(5), N1–Sn1–P1 75.91(4), N2–Sn1–P1 95.92(4), N1–Sn1–P2 160.46(4).

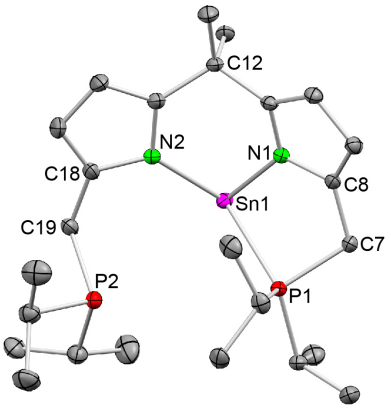

Fig. 3 XRD molecular structure of stannylene **4** (40% displacement ellipsoids, H atoms have been omitted for clarity). Selected bond lengths (Å) and angles (°): Sn1–N1 2.146(2), Sn1–N2 2.157(2), Sn1–P1 2.7378(5), Sn1···P2 3.7626(7); N1–Sn1–N2 83.87(7), N1–Sn1–P1 72.94(5), N2–Sn1–P1 111.76(5), N1–Sn1–P2 122.43(5).

The XRD molecular structure of distannylene **5** is shown in Fig. 4. In it, each $pyrmP^iPr_2$ fragment of the tetradentate $(pyrmP^iPr_2)_2CMe_2$ ligand is attached through the N and P atoms to the Sn atom of an $Sn\{N(SiMe_3)_2\}$ moiety. Overall, the molecule displays a C_2 symmetry (non-crystallographic) with the two-fold axis passing through the bridgehead C12 atom.

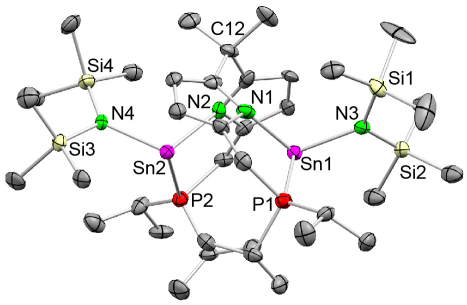

Fig. 4 XRD molecular structure of distannylene **5** (25% displacement ellipsoids, H atoms have been omitted for clarity. Only one of the two independent but analogous molecules found in the asymmetric unit is shown). Selected bond lengths (Å) and angles (°): Sn1–N1 2.18(2), Sn1–N3 2.15(2), Sn2–N2 2.22(2), Sn2–N4 2.15(1), Sn1–P1 2.797(5), Sn2–P2 2.816(5), Sn1···Sn2 3.930(2); N1–Sn1–N3 106.7(6), N1–Sn1–P1 75.2(4), N3–Sn1–P1 94.8(4), N2–Sn2–N4 105.8(6), N2–Sn2–P2 75.2(5), N4–Sn2–P2 96.9(4).

As occurred with the germanium analogue,[12] the solid-state structure of **3** is not maintained in solution. In fact, at room temperature, its ^1H, $^{13}C\{^1H\}$ and $^{31}P\{^1H\}$ NMR spectra indicate that both $HpyrmP^tBu_2$ fragments are equivalent. A variable temperature $^{31}P\{^1H\}$ NMR study (SI, Figure S12) revealed the existence in solution of a fluxional process that equilibrates the two $HpyrmP^tBu_2$ fragments of **3**. Only one signal was seen above 193 K, while the signals of two inequivalent P atoms could only be observed below 165 K. The low coalescence temperature, *ca.* 173 K, indicated a facile dynamic process ($\Delta G^{\ddagger}$ *ca.* 6.9 kcal mol^{-1}). The reversible equilibria depicted in Scheme 3, by which the "pendant" and "bonded" phosphane fragments of stannylene **3** are exchanged, may explain the observed fluxional behavior. The $\Delta G^{\ddagger}$ value reported for the analogous Ge system is 2.0 kcal mol^{-1} greater than that of **3**.[12] These data confirm a hemilabile behavior for the *P*-donor groups, a fact that can be very beneficiary in reactivity/catalysis.

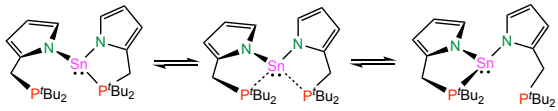

Scheme 3 Proposed equilibria to account for the fluxional behavior of stannylene **3** in solution.

Stannylene **4** is also fluxional in solution but, in this case, we observed only one $^{31}P\{^1H\}$ NMR resonance even at 150 K, which is the limiting low temperature allowed by the used solvent (1:1 toluene/dichloromethane-d_2). Therefore, the fluxional process involving **4** has an activation barrier even lower than that of **3**.

The room temperature $^{31}P\{^1H\}$ NMR spectra of **1**–**5** revealed that the $^1J_{^{31}P\text{-}^{119}Sn}$ coupling constants of stannylenes **1** (1563 Hz) and **2** (1711 Hz), which contain "normal" non-dynamic Sn–P interactions, are much larger than those of the stannylenes that participate in equilibria (**5**; 831 Hz) or in fluxional processes (**3** and **4**; 655 and 968 Hz, respectively). The reported $^1J_{^{31}P\text{-}^{119}Sn}$ coupling constants for the PSnP stannylenes **A**[16] and **B**,[11] which are not fluxional in solution, are 647 and 1355 Hz, respectively, in agreement with their above-commented long (**A**) and short (**B**) Sn–P bond distances.

Prior to exploring the coordination chemistry of stannylenes **3** and **4**, we decided to perform some density functional theory/natural bond orbital (DFT/NBO) calculations aimed at shedding light on the nature of the frontier molecular orbitals of **3**

and **4** and the availability of the P and Sn lone pairs (LPs) for further coordination. Calculations at the BP86-D3/def2-SVP level showed that the LUMO of both compounds is constituted by a p orbital of the Sn atom, while the LPs of the Sn and pendant P atoms are located in HOMO–5 (**3**: 89.4% s, 10.6% p; **4**: 89.3% s, 10.7% p) and HOMO–4 (**3**: 52.6% s 47.4% p; **4**: 52.5% s, 47.5% p), respectively (ESI, Figure S32), corroborating that, despite being donor-stabilized stannylenes, compounds **3** and **4** maintain the ambiphilic character (dual Lewis acid/base behavior) typical of non-stabilized heavier tetrylenes.[4g] The NBO second-order perturbation theory (SOPT) approach applied to stannylene **3** revealed a weak donor-acceptor interaction ($\Delta E^{(2)}$ = –4.51 kcal mol^{-1}) between the pendant phosphane LP and an empty σ*(Sn–N) orbital, accounting for the "contact" found by XRD between the Sn and that P atom (Sn1···P2 3.555 Å), but the analogous interaction in stannylene **4** is much weaker ($\Delta E^{(2)}$ = –0.56 kcal mol^{-1}), consistent with a longer Sn1···P2 distance (3.763 Å).

Having in mind that only two reports aimed at preparing PSnP pincer complexes have hitherto been published (they use the PSnP stannylenes **A** and **B**, Figure 1),[16,11] in order to establish the coordination properties of stannylenes **3** and **4** and looking for new PSnP pincer complexes, we decided to study their reactivity with [$PdCl_2(MeCN)_2$], [AuCl(tht)] (tht = tetrahydrothiophene) and [Pd(η^3-C_3H_5)(η^5-C_5H_5)] (C_3H_5 = allyl; C_5H_5 = cyclopentadienyl). The new results would also allow us to establish the analogies/differences between the reactivities of **3** and **4** and those of their germanium counterparts.

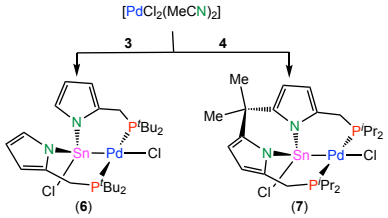

Scheme 4 Reactivity of [$PdCl_2(MeCN)_2$] with stannylenes **3** and **4**.

Both **3** and **4** reacted readily with [$PdCl_2(MeCN)_2$] in toluene at room temperature to give the chloridostannyl palladium(II) derivatives [PdCl{κ^3*P*,*Sn*,*P*-SnCl(HpyrmP^{t}Bu$_2$)$_2$}] (**6**) and [PdCl{κ^3*P*,*Sn*,*P*-SnCl(pyrmP^{i}Pr$_2$)$_2$CMe$_2$}] (**7**), respectively (Scheme 4). The C_S symmetric structures suggested by NMR (^{1}H, ^{13}C{^{1}H} and ^{31}P{^{1}H}) for these complexes, which indicated equivalent pyrrole rings and phosphane groups and also showed inequivalent methyls for the CMe_2 group of **7**, were confirmed by XRD. The molecular structures (Fig. 5 and 6) clearly show that the insertion of the stannylene Sn atom into a Cl–Pd bond of the metal precursor is a key step in the reactions of **3** and **4** with [$PdCl_2(MeCN)_2$], as they rendered square-planar palladium(II) complexes having a PSnP pincer chloridostannyl ligand. Both structures are closely related, being the Sn–Cl, Sn–Pd and Pd–P bond distances very similar in both compounds, although the dihedral angle between the planes defined by their pyrrole rings is 169.1(3)° for **6** but 128.8(2)° for **7**. These structures are reminiscent of those of their germanium counterparts, but their Sn–Pd distances are *ca.* 0.17 Å longer than the corresponding Ge–Pd distances.[12,19a] DFT/NBO calculations showed that the contribution of the Sn atom to the Sn–Pd σ-bond is smaller in **6** [49.7% Sn (sp$^{0.26}$) + 50.3% Pd (sd$^{10.14}$); WBI = 0.47] than in **7** [61.0% Sn (sp$^{0.66}$) + 39.0% Pd (sd$^{1.08}$); WBI = 0.46].

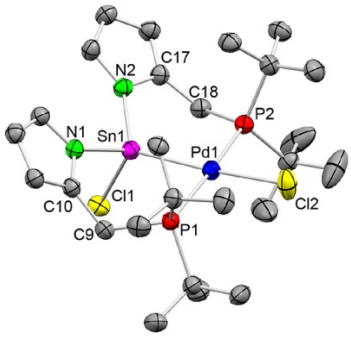

Fig. 5 XRD molecular structure of complex **6** (25% displacement ellipsoids, H atoms have been omitted for clarity). Selected bond lengths (Å) and angles (°): Pd1–P1 2.388(1), Pd1–P2 2.383(1), Pd1–Sn1 2.4712(4), Pd1–Cl2 2.361(1), Sn1–Cl1 2.383(1), Sn1–N1 2.066(3), Sn1–N2 2.052(3); N1–Sn1–N2 105.0(1), N1–Sn1–Pd1 116.51(9), N2–Sn1–Pd1 118.5(1), N1–Sn1–Cl1 99.1(1), N2–Sn1–Cl1 99.7(1), Cl1–Sn1–Pd1 115.12(3), Sn1–Pd1–Cl2 174.84(6), P1–Pd1–P2 171.76(4), P1–Pd1–Sn1 86.74(3), P2–Pd1–Sn1 87.30(3), P1–Pd1–Cl2 92.97(4), P2–Pd1–Cl2 93.47(4).

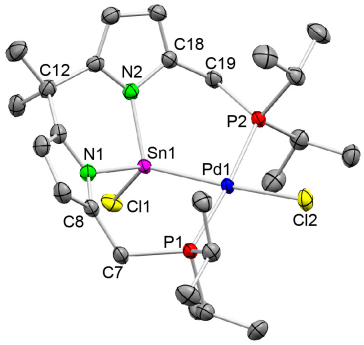

Fig. 6 XRD molecular structure of complex **7** (40% displacement ellipsoids, H atoms have been omitted for clarity). Selected bond lengths (Å) and angles (°): Pd1–Sn1 2.4602(3), Pd1–P1 2.3475(7), Pd1–P2 2.3500(7), Pd1–Cl2 2.3604(7), Sn1–Cl1 2.3632(7), Sn1–N1 2.051(2), Sn1–N2 2.051(3); N1–Sn1–N2 92.1(1), N1–Sn1–Pd1 114.14(7), N2–Sn1–Pd1 114.61(7), N1–Sn1–Cl1 103.96(7), N2–Sn1–Cl1 103.62(7), Cl1–Sn1–Pd1 123.45(2), Sn1–Pd1–Cl2 174.07(2), P1–Pd1–P2 174.94(2), P1–Pd1–Sn1 87.48(2), P2–Pd1–Sn1 87.47(2), P1–Pd1–Cl2 91.78(3), P2–Pd1–Cl2 93.25(3).

The reactions of **3** and **4** with [AuCl(tht)] (tht = tetrahydrothiophene) also proceeded gently in THF at room temperature. However, while that of **3** afforded a single product, subsequently identified as [Au{κ^3*P*,*Sn*,*P*-SnCl(HpyrmP^{t}Bu$_2$)$_2$}] (**8**; Scheme 5), the reaction of **4** gave some metallic gold (violet solid) and a mixture of products that could not be separated and identified.

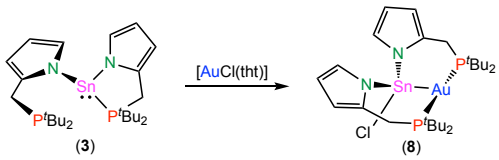

Scheme 5 Reaction of stannylene **3** with [AuCl(tht)].

The NMR spectra of **8** indicated a C_S symmetric structure and the absence of tht in the molecule. As no single crystals of **8** could be prepared and as the reaction of [AuCl(tht)] with the germanium analogue of **3** has been reported to afford an interesting T-shaped PGeP-pincer chloridogermyl gold(I)

complex,[12] we used DFT methods to obtain the molecular structure of complex **8** (Fig. 7). Complex **8** also shows an unusual T-shaped ligand arrangement around the Au atom,[21] but, remarkably, the Sn–Au distance, 3.120 Å, much longer than the Ge–Au distance of the germanium analogue (2.764 Å) and the environment around the Sn atom is far from being tetrahedral, as the Cl–Sn–Au angle is 161.8º (that of the germanium analogue is 156.7º). SOPT/NBO calculations proposed that the Sn–Au interaction is due to two weak donor–acceptor interactions, LP(Sn) → σ*(Au–P) ($\Delta E^{(2)}$ = –9.0 kcal mol^{-1}) and LP(Au) → σ*(Sn–Cl) ($\Delta E^{(2)}$ = –2.3 kcal mol^{-1}), which agree with the small WBI computed for this bond, 0.10. Nevertheless, a Quantum Theory of Atoms in Molecules (QTAIM) calculation (ESI, Table S2) was able to find a bond critical point between the Sn and Au atoms, yet with a very small electron density, ρ(r) = 0.027 e Å^3. The positive charges of the Sn and Au atoms, +0.94 and +0.21, respectively, tend to separate the corresponding atoms and may account, at least in part, for the long Sn–Au distance. Therefore, the Sn atom of **8** is less prone to bind the Au atom than the Ge atom of the germanium analogue, most probably because the Sn LP of **8** has a greater s character and a larger volume than the corresponding Ge LP.

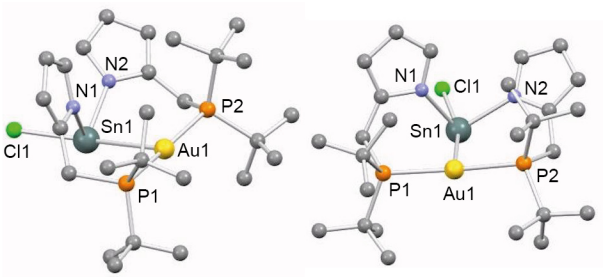

Fig. 7 Two views of the DFT-optimized structure of complex **8** (H atoms have been omitted for clarity). Selected bond lengths (Å) and angles (º): Au1–Sn1 3.120, Au1–P1 2.364, Au1–P2 2.355, Sn1–Cl1 2.459, Sn1–N1 2.261, Sn1–N2 2.221; N1–Sn1–N2 92.1, N1–Sn1–Au1 71.4, N2–Sn1–Au1 93.9, N1–Sn1–Cl1 91.8, N2–Sn1–Cl1 93.7, Cl1–Sn1–Au1 161.8, P1–Pd1–P2 171.2, P1–Au1–Sn1 93.2, P2–Au1–Sn1 93.6.

The reactions of **3** and **4** with [Pd(η^3-C_3H_5)(η^5-C_5H_5)], which has been recognized as a convenient precursor to palladium(0) complexes (by facile reductive elimination of allylcyclopentadiene),[22] were instantaneous in toluene at room temperature. In this case, **3** gave a mixture of products that could not be separated and identified, whereas **4** afforded [Pd{κ^3*P*,*Sn*,*P*-Sn(pyrmP^{i}Pr$_2$)$_2$CMe$_2$}] (**9**; Scheme 6).

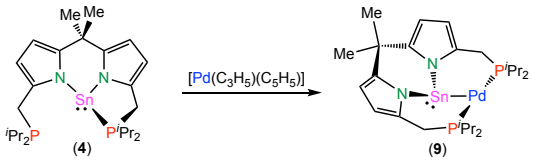

Scheme 6 Synthesis of complex **9**.

Although **9** contains a stannylene instead of a chloridostannyl ligand, its ^{1}H, ^{13}C{^{1}H} and ^{31}P{^{1}H} NMR spectra are comparable to those of complex **7**, indicating C_S symmetry. Its molecular structure (Fig. 8), which was deduced by DFT calculations, resembles that of complex **7**, but **9** has no Cl atoms and its Sn–Pd distance, 2.660 Å, is 0.20 Å longer than that of **7**. Therefore, **9** is a rare example of a T-shaped palladium(0) complex.[19a,23] SOPT/NBO calculations indicated that the bonding between the Sn and Pd atoms is mainly constituted by two donor–acceptor interactions, that is, a rather strong LP(Pd) → p(Sn) ($\Delta E^{(2)}$ = –21.5 kcal mol^{-1}) and a weaker LP(Sn) → σ*(Pd–P) ($\Delta E^{(2)}$ = –11.0 kcal mol^{-1}). In this case, the computed WBI of the Sn–Pd bond (0.49) is comparable to those of **6** (0.47) and **7** (0.46) but larger than that of the T-shaped gold(I) complex **8** (0.10). The QTAIM electron density at the Sn–Pd bond critical point was found to be 0.047 e Å^{-3}. Therefore, the stannylene fragment of complex **9** belongs to the yet small family of *Z*-type (σ-acceptor) ligands,[24,25] as it receives electron density from a filled d orbital of the Pd atom into an empty p orbital of the Sn atom. A similar situation has been found for the germanium analogue of complex **9**, but in that case the Ge–Pd bond distance is 2.507 Å.[19a] A platinum(0) complex derived from stannylene **B** (Fig. 1) is the only previously known complex containing a PSnP pincer stannylene, but its stannylene fragment behaves as a "normal" 2-electron-donor ligand.[11] A *Z*-ligand behavior of a stannylene has been rarely observed.[25]

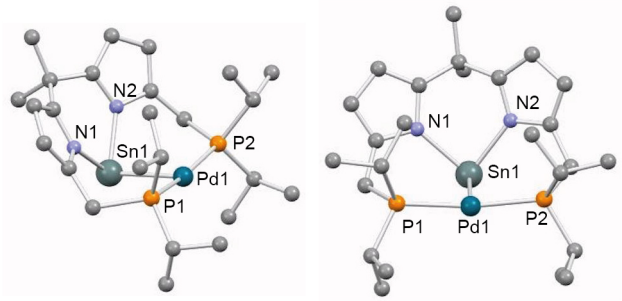

Fig. 8 Two views of the DFT-optimized structure of complex **9** (H atoms have been omitted for clarity). Selected bond lengths (Å) and angles (º): Pd1–P1 2.326, Pd1–P2 2.325, Pd1–Sn1 2.660, Sn1–N1 2.200, Sn1–N2 2.195; N1–Sn1–N2 84.5, N1–Sn1–Pd1 71.4, N2–Sn1–Pd1 95.7, P1–Pd1–P2 169.2, P1–Pd1–Sn1 91.8, P2–Pd1–Sn1 92.7.

Conclusions

The new PSnP stannylenes **3** and **4** have been successfully prepared and characterized and their behavior as ligands has started to be investigated.

It has been found that the coordination chemistry of stannylenes **3** and **4** follows reaction pathways that are rather similar to those followed by the analogous germylenes, but the resulting Sn–M bonds are considerably longer (and weaker) than the corresponding Ge–M bonds. This observation is expected to induce profound differences in the reactivity of these compounds.

A T-shaped palladium(0) complex containing a PSnP pincer-type stannylene ligand (compound **9**) has been prepared from **4** and [Pd(η^3-C_3H_5)(η^5-C_5H_5)]. Interestingly, the stannylene fragment of this complex behaves as a *Z*-type (σ-acceptor) ligand, a coordination mode that is rare in the transition metal chemistry of stannylenes.

No doubt, the results reported in this article will stimulate the synthesis of many more PSnP pincer transition metal

complexes with interesting structural, bonding, magnetic, and/or catalytic properties.

Experimental section

General data

All reactions and product manipulations were carried out under argon in a drybox or using Schlenk-vacuum line techniques. Solvents were dried over appropriate desiccating reagents and were distilled under argon immediately before use. The compounds $H_2pyrmP^tBu_2$,[12] $(HpyrmP^iPr_2)_2CMe_2$,[13] [AuCl(tht)],[26] $[Pd(\eta^3\text{-}C_3H_5)(\eta^5\text{-}C_5H_5)]$[27] and $Sn\{N(SiMe_3)_2\}_2$[28] were prepared following published procedures. All remaining reagents were purchased from commercial sources and were stored under argon in a drybox. All reaction products were vacuum-dried for several hours prior to being weighted and analyzed. NMR spectra were run on Bruker NAV-400, AV-400 and AC-300 instruments, using as standards the residual protic solvent resonance for ^1H [$\delta(C_6HD_5)$ 7.16 ppm; $\delta(CHDCl_2)$ 5.32 ppm], the solvent resonance for ^{13}C [$\delta(C_6D_6)$ 128.10 ppm; $\delta(CD_2Cl_2)$ 54.00 ppm], external 85% aqueous H_3PO_4 for ^{31}P (δ 0.00 ppm) and external $SnMe_4$ in $CDCl_3$ for ^{119}Sn (δ 0.00 ppm). Microanalyses were obtained with a FlashEA112 (Thermo-Finnigan) microanalyzer, except for the products that were very unstable towards air and/or moisture.

Synthetic procedures and characterization data

$SnCl(HpyrmP^tBu_2)$ (1): A Schlenk tube, previously charged with a 0.3 *M* solution of $H_2pyrmP^tBu_2$ in toluene (3.85 mL, 1.16 mmol) and diethyl ether (2 mL), was cooled to –78 ºC. A subsequent addition of a 1.6 *M* solution of BuLi in hexanes (0.75 mL, 1.20 mmol) resulted in a bright yellow solution that was allowed to reach the room temperature and then it was stirred for 4 h. The Schlenk tube was then transferred to a drybox. Solid $SnCl_2$ (190 mg, 1.00 mmol) was added and the resulting pale pink suspension was stirred for 18 h. Solvents were removed under vacuum and the residue was extracted into toluene (4 x 10 mL; solution decanted). The combined toluene extracts were evaporated to dryness and the residue was washed with hexane (2 x 2 mL) to give **1** as an orange solid (182 mg, 48%). ^1H NMR (C_6D_6, 400.1 MHz, 298 K): δ 7.00 (br s, 1 H, 1 C*H* of Hpyr), 6.54 (t, $J_{H\text{-}H}$ = 2.6 Hz, 1 H, 1 C*H* of Hpyr), 6.34 (br s, 1 H, 1 C*H* of Hpyr), 3.04 (br s, 2 H, 2 C*H* of PCH_2), 0.88 (s, 9 H, 3 CH_3 of ^{t}Bu), 0.86 (s, 9 H, 3 CH_3 of ^{t}Bu) ppm. $^{13}C\{^1H\}$ NMR (C_6D_6, 100.6 MHz, 298 K): δ 136.2 (d, $J_{C\text{-}P}$ = 4.1 Hz, *C* of Hpyr), 124.9 (d, $J_{C\text{-}P}$ = 4.4 Hz, *C*H of Hpyr), 111.5 (s, *C*H of Hpyr), 107.1 (d, $J_{C\text{-}P}$ = 7.4 Hz, *C*H of Hpyr), 35.5 (br s, *C* of ^{t}Bu), 29.2 (s, *C*H_3 of ^{t}Bu), 21.1 (d, $J_{C\text{-}P}$ = 9.1 Hz, P*C*H_2) ppm. $^{31}P\{^1H\}$ NMR (C_6D_6, 162.1 MHz, 298 K): δ 54.0 (s, sat, $J_{P\text{-}117Sn}$ = 1493 Hz, $J_{P\text{-}119Sn}$ = 1563 Hz) ppm. $^{119}Sn\{^1H\}$ NMR (C_6D_6, 149.2 MHz, 298 K): δ –98.2 (d, $J_{119Sn\text{-}P}$ = 1563 Hz) ppm.

$Sn\{N(SiMe_3)_2\}(HpyrmP^tBu_2)$ (2): A toluene solution of $H_2pyrmP^tBu_2$ (2.80 mL, 0.36 *M*, 1.00 mmol) was added to a solution of $Sn\{N(SiMe_3)_2\}_2$ (440 mg, 1.00 mmol) in THF (4 mL). The Schlenk tube was then transferred to an oil bath preheated at 60 ºC. After 18 h, the reaction mixture was cooled down to room temperature and all volatiles were removed under vacuum to give **2** as a pale orange solid (448 mg, 89%). ^1H NMR (C_6D_6, 400.5 MHz, 298 K): δ 6.97 (s, 1 H, 1 C*H* of Hpyr), 6.47 (s, 1 H, 1 C*H* of Hpyr), 6.29 (s, 1 H, 1 C*H* of Hpyr), 3.06 (d, $J_{H\text{-}P}$ = 8.1 Hz, 2 H, 2 C*H* of PCH_2), 1.04 (s, 9 H, 3 CH_3 of ^{t}Bu), 1.01 (s, 9 H, 3 CH_3 of ^{t}Bu), 0.36 (s, 18 H, 6 CH_3 of $N(SiMe_3)_2$) ppm. $^{13}C\{^1H\}$ NMR (C_6D_6, 100.7 MHz, 298 K): δ 136.0 (d, $J_{C\text{-}P}$ = 5.7 Hz, *C* of Hpyr), 125.4 (d, $J_{C\text{-}P}$ = 6.2 Hz, *C*H of Hpyr), 111.4 (s, *C*H of Hpyr), 107.6 (d, $J_{C\text{-}P}$ = 8.0 Hz, *C*H of Hpyr), 35.3 (br s, *C* of ^{t}Bu), 29.5 (s, *C*H_3 of ^{t}Bu), 19.0 (d, $J_{C\text{-}P}$ = 5.2 Hz, P*C*H_2), 6.2 (s, *C*H_3 of $N(SiMe_3)_2$) ppm. $^{31}P\{^1H\}$ NMR (C_6D_6, 162.1 MHz, 298 K): δ 41.7 (s, sat, $J_{P\text{-}117Sn}$ = 1627 Hz, $J_{P\text{-}119Sn}$ = 1711 Hz) ppm. $^{119}Sn\{^1H\}$ NMR (C_6D_6, 149.2 MHz, 298 K): δ –17.3 (d, $J_{119Sn\text{-}P}$ = 1711 Hz) ppm.

$Sn(HpyrmP^tBu_2)_2$ (3): *Method (a):* A solution of BuLi in hexanes (1.4 mL, 1.6 *M*, 2.24 mmol) was dropwise added to a solution prepared by adding $H_2pyrmP^tBu_2$ (5.5 mL of a 0.37 *M* solution in toluene, 2.04 mmol) to diethyl ether (1 mL). After stirring for 3 h, a suspension of $SnCl_2$ (190 mg, 1.00 mmol) in diethyl ether (1 mL) was added and the resulting brown suspension was stirred for 18 h. The solvent was removed under reduced pressure and the residue was extracted into 1:1 hexanes/toluene (4 x 4 mL; solution decanted). The combined extracts were evaporated to dryness and the solid residue was washed with hexanes (2 x 1 mL) to give **3** as a pale orange solid (385 mg, 67%). *Method (b):* A toluene solution of $H_2pyrmP^tBu_2$ (2.80 mL, 0.36 *M*, 1.00 mmol) was added to a solution of $Sn\{N(SiMe_3)_2\}_2$ (220 mg, 0.50 mmol) in THF (4 mL). The resulting clear orange solution was then heated at 60 ºC for 18 h. The reaction mixture was allowed to cool down to room temperature and all volatiles were removed under vacuum to give **3** as a pale orange solid (476 mg, 94%). Anal. (%) Calcd. for $C_{26}H_{46}N_2P_2Sn$ (*M* = 567.32): C, 55.05; H, 8.17; N, 4.94; found: C, 54.31; H, 7.99; N, 4.78. ^1H NMR (C_6D_6, 300.1 MHz, 298 K): δ 6.87 (br s, 1 H, C*H* of Hpyr), 6.54 (br s, 1 H, C*H* of Hpyr), 6.41 (br s, 1 H, C*H* of Hpyr), 3.11 (br s, 2 H, P*C*H_2), 1.04 (s, 9 H, 3 CH_3 of ^{t}Bu), 1.02 (s, 9 H, 3 CH_3 of ^{t}Bu) ppm. $^{13}C\{^1H\}$ NMR (C_6D_6, 100.7 MHz, 298 K): δ 135.8 (d, $J_{C\text{-}P}$ = 7.4 Hz, *C* of Hpyr), 126.0 (s, *C*H of Hpyr), 110.4 (s, *C*H of Hpyr), 108.8 (s, *C*H of Hpyr), 33.7 (d, $J_{C\text{-}P}$ = 10.8 Hz, *C* of ^{t}Bu), 29.8 (s, *C*H_3 of ^{t}Bu), 22.1 (d, $J_{C\text{-}P}$ = 5.4 Hz, P*C*H_2) ppm. $^{31}P\{^1H\}$ NMR (C_6D_6, 121.5 MHz, 298 K): δ 36.7 (s, sat, $J_{P\text{-}117Sn}$ = 625 Hz, $J_{P\text{-}119Sn}$ = 655 Hz) ppm.

$Sn(pyrmP^iPr_2)_2CMe_2$ (4): A toluene solution of $(HpyrmP^iPr_2)_2CMe_2$ (2.2 mL, 0.45 *M*, 1.00 mmol) was added to a Schlenk tube containing $Sn\{N(SiMe_3)_2\}_2$ (467 g, 1.10 mmol). The bright orange solution was stirred at 60 ºC for 16 h. After cooling the reaction mixture at room temperature, a small amount of solid precipitated. The solution was decanted and evaporated to dryness and the solid residue was washed with hexane (4 x 2 mL) to give **4** as an off-white solid (185 mg, 34%). Anal. (%) Calcd. for $C_{25}H_{42}N_2P_2Sn$ (*M* = 551.27): C, 54.47; H, 7.68; N, 5.08; found: C, 54.25; H, 7.59; N, 4.83. ^1H NMR (C_6D_6, 400.1 MHz, 298 K): δ 6.40 (d, $J_{H\text{-}H}$ = 4.0 Hz, 2 H, 2 C*H* of 2 pyr), 6.24 (d, $J_{H\text{-}H}$ = 4.0 Hz, 2 H, 2 C*H* of 2 pyr), 2.87 (s, 4 H, 2 CH_2P), 1.97 (s, 6 H, C*Me*$_2$), 1.63 (m, 4 H, 4 C*H* of 4 $CHMe_2$), 0.83 (br s, 24 H, 8 CH_3 of 4 $CHMe_2$) ppm. $^{13}C\{^1H\}$ NMR (C_6D_6, 100.6 MHz, 298 K): δ 146.1 (s, *C* of pyr), 131.1 (s, *C* of pyr), 106.7 (s, *C*H of pyr), 103.6 (s, *C*H of pyr), 37.7 (s, C*Me*$_2$), 24.3 (br s, *C*H_2P), 22.2 (s, *C*Me_2), 19.3 (s, *C*H of $CHMe_2$), 18.5 (s, *C*H_3 of $CHMe_2$) ppm. $^{31}P\{^1H\}$ NMR (C_6D_6,

121.5 MHz, 298 K): δ 14.4 (s, sat, $J_{P\text{-}117Sn}$ = 927 Hz, $J_{P\text{-}119Sn}$ = 968 Hz) ppm.

$Sn_2\{N(SiMe_3)_2\}_2\{(pyrmP^iPr_2)_2CMe_2\}$ (5): $Sn\{N(SiMe_3)_2\}_2$ (28 mg, 0.06 mmol) was added to a solution of stannylene **4** (33 mg, 0.06 mmol) in C_6D_6 (1 mL) contained in a J. Young NMR tube. The resulting bright orange solution was heated at 60 ºC and the reaction was monitorized by NMR. The transformation of **4** into **5** was progressively observed. After 36 h, the **4**/**5** molar ratio was 1/0.3. Some more $Sn\{N(SiMe_3)_2\}_2$ (28 mg, 0.06 mmol) was added and the NMR tube was further heated at 60 ºC for 72 h. At this point, the **4**/**5** molar ratio was 1/2.5. After one additional week at room temperature, a 1/4/5 molar mixture of **4**, **5** and $Sn\{N(SiMe_3)_2\}_2$ was observed. The solution was evaporated to dryness and the residue was extracted with hexanes (2 mL). Cooling the extract to –18 ºC for 16 h led to the precipitation of a few colorless crystals suitable for X-ray diffraction. The following NMR data of **5** were taken from spectra of a sample containing a 1/4/5 mixture of **4**, **5** and $Sn\{N(SiMe_3)_2\}_2$. ^{1}H NMR (C_6D_6, 300.1 MHz, 298 K): δ 6.64 (br s, 2 H, 2 C*H* of 2 pyr), 6.17 (br s, 2 H, 2 C*H* of 2 pyr), 3.98 (d, $J_{H\text{-}P}$ = 15.0 Hz, 2 H, 2 C*H* of 2 CH_2P), 2.76 (d, $J_{H\text{-}P}$ = 15.0 Hz, 2 H, 2 C*H* of 2 CH_2P), 1.99 (s, 6 H, C*Me*$_2$), 1.87–0.88 (m, 24 H, 8 CH_3 of 4 $CHMe_2$), 0.47 (br s, 6 CH_3 of 2 $N(SiMe_3)_2$), 0.36 (br s, 6 CH_3 of 2 $N(SiMe_3)_2$) ppm. ^{31}P{^{1}H} NMR (C_6D_6, 121.5 MHz, 298 K): δ 2.9 (s, sat, $J_{P\text{-}117Sn}$ = 791 Hz, $J_{P\text{-}119SSn}$ = 831 Hz) ppm.

[PdCl{κ^3*P*,*Sn*,*P*-SnCl(HpyrmP^{t}Bu$_2$)$_2$}] (6): Toluene (3 mL) was added to a mixture of stannylene **3** (34 mg, 0.06 mmol) and $[PdCl_2(MeCN)_2]$ (16 mg, 0.06 mmol). The reaction mixture was stirred at room temperature for 4 h. The initial orange suspension changed to a dark orange solution. The solvent was evaporated to give a sticky solid that was washed with hexanes (4 x 2 mL) to render **6** as a pale brown solid (12 mg, 27%). Anal. (%) Calcd. for $C_{26}H_{46}Cl_2N_2P_2PdSn$ (*M* = 744.64 amu): C, 41.94 H, 6.23; N, 3.76; found: C, 40.25; H, 5.10; N 3.61 (although these results, possibly affected by the air-sensitivity of this compound, are outside the accepted range of analytical purity, they are provided to illustrate the best values obtained to date). ^{1}H NMR (C_6D_6, 400.1 MHz, 298 K): δ 7.40 (br s, 2 H, 2 CH of 2 Hpyr), 6.50 (t, $J_{H\text{-}H}$ = 2.9 Hz, 2 H, 2 C*H* of 2 Hpyr), 6.23 (br s, 2 H, 2 C*H* of 2 Hpyr), 3.34 (br s, 4 H, 4 C*H* of 2 PCH_2), 1.32 (vt, $J_{H\text{-}P}$ = 8.0 Hz, 18 H, 6 CH_3 of 2 ^{t}Bu), 1.23 (vt, $J_{H\text{-}P}$ = 8.0 Hz, 18 H, 6 CH_3 of 2 ^{t}Bu) ppm. ^{13}C{^{1}H} NMR (C_6D_6, 100.6 MHz, 298 K): δ 131.3 (s, *C* of Hpyr), 125.4 (d, $J_{C\text{-}P}$ = 17.3 Hz, *C*H of Hpyr), 111.8 (s, *C*H of Hpyr), 111.0 (m, *C*H of Hpyr), 39.3 (vt, $J_{C\text{-}P}$ = 8.1 Hz, *C* of ^{t}Bu), 38.7 (vt, $J_{C\text{-}P}$ = 8.1 Hz, *C* of ^{t}Bu), 30.6 (d, $J_{C\text{-}P}$ = 10.9 Hz, *C*H$_3$ of ^{t}Bu), 30.1 (d, $J_{C\text{-}P}$ = 10.9 Hz, *C*H$_3$ of ^{t}Bu), 24.6 (vt, $J_{C\text{-}P}$ = 11.1 Hz, *C*H$_2$ of PCH_2) ppm.^{31}P{^{1}H} NMR (C_6D_6, 162.1 MHz, 298 K): δ 38.4 (s, sat, $J_{P\text{-}119Sn}$ = 195 Hz) ppm. ^{119}Sn{^{1}H} NMR (C_6D_6, 149.2 MHz, 298 K): δ –147.1 (t, $J_{119Sn\text{-}P}$ = 195 Hz) ppm

[PdCl{κ^3*P*,*Sn*,*P*-SnCl(pyrmP^{i}Pr$_2$)$_2$CMe$_2$}] (7): A toluene (2 mL) solution of $[PdCl_2(MeCN)_2]$ (16 mg, 0.06 mmol) was mixed with a toluene (2 mL) solution of stannylene **4** (29.5 mg, 0.05 mmol). The reaction mixture was stirred at room temperature for 16 h to give a brownish-orange suspension. The solvent was vacuum-dried and the solid residue was washed with hexanes (5 x 2 mL) to give **7** as a brown solid (20 mg, 55%). Anal. (%) Calcd. for $C_{25}H_{42}Cl_2N_2P_2PdSn$ (*M* = 728.60): C, 41.21; H, 5.81; N, 3.84; found: C, 41.93; H, 5.12; N, 3.43 (although these results, possibly affected by the air-sensitivity of this compound, are outside the accepted range of analytical purity, they are provided to illustrate the best values obtained to date). ^{1}H NMR (C_6D_6, 400.1 MHz, 298 K): δ 6.26 (d, $J_{H\text{-}H}$ = 4.0 Hz, 2 H, 2 C*H* of 2 pyr), 6.04 (d, $J_{H\text{-}H}$ = 4.0 Hz, 2 H, 2 C*H* of 2 pyr), 3.06 (dd, $J_{H\text{-}H}$ = 16.0 Hz, $J_{H\text{-}P}$ = 8.0 Hz, 2 H, 2 C*H* of 2 CH_2P), 2.69 (d, $J_{H\text{-}H}$ = 16.0 Hz, 2 H, 2 C*H* of 2 CH_2P), 2.58 (m, 2 H, 2 C*H* of 2 $CHMe_2$), 2.04 (s, 3 H, CH_3 of CMe_2), 1.95 (m, 2 H, 2 C*H* of 2 $CHMe_2$) 1.84 (s, 3 H, CH_3 of CMe_2), 1.29 (dd, $J_{H\text{-}P}$ = 16.0 Hz, $J_{H\text{-}H}$ = 8.0 Hz, 6 H, 2 CH_3 of 2 $CHMe_2$), 0.91-1.04 (m, 12 H, 4 CH_3 of 4 $CHMe_2$), 0.70 (dd, $J_{H\text{-}P}$ = 16.0 Hz, $J_{H\text{-}H}$ = 8.0 Hz, 6 H, 2 CH_3 of 2 $CHMe_2$) ppm. ^{13}C{^{1}H} NMR (C_6D_6, 100.7 MHz, 298 K): δ 149.0 (s, *C* of pyr), 130.8 (s, *C* of pyr), 109.2 (s, *C*H of pyr), 105.8 (s, *C*H of pyr), 37.7 (s, *C*Me$_2$), 36.0 (s, *C*H$_3$ of C*Me*$_2$), 26.5 (vt, $J_{C\text{-}P}$ = 11.1 Hz, *C*H of $CHMe_2$), 26.3 (vt, $J_{C\text{-}P}$ = 11.1 Hz, *C*H of $CHMe_2$), 25.4 (s, *C*H$_3$ of C*Me*$_2$), 23.1 (vt, $J_{C\text{-}P}$ = 11.1 Hz, *C*H$_2$P), 19.6 (s, *C*H$_3$ of $CHMe_2$), 19.3 (s, *C*H$_3$ of $CHMe_2$), 19.2 (s, *C*H$_3$ of $CHMe_2$), 16.9 (s, *C*H$_3$ of $CHMe_2$) ppm. ^{31}P{^{1}H} NMR (C_6D_6, 162.1 MHz, 298 K): δ 37.9 (s, sat, $J_{P\text{-}117Sn}$ = 156 Hz, $J_{P\text{-}119Sn}$ = 165 Hz) ppm. ^{119}Sn{^{1}H} NMR (CD_2Cl_2, 149.2 MHz, 298 K): δ –68.7 (t, $J_{119Sn\text{-}P}$ = 165 Hz) ppm.

[Au{κ^3*P*,*Sn*,*P*-SnCl(HpyrmP^{t}Bu$_2$)$_2$}] (8): THF (4 mL) was added to a mixture of compound **3** (34 mg, 0.06 mmol) and [AuCl(tht)] (19 mg, 0.06 mmol). The initial orange color did not change. The reaction mixture was stirred at room temperature for 12 h and was vacuum-dried to give a sticky solid that was washed with hexanes (2 x 2 mL) to render **8** as a brownish orange solid (45 mg, 94%). Anal. (%) Calcd. for $C_{26}H_{46}AuClN_2P_2Sn$ (*M* = 799.73): C, 39.05; H, 5.80; N, 3.50; found: C, 38.16; H, 5.46; N 3.32 (although these results, possibly affected by the air-sensitivity of this compound, are outside the accepted range of analytical purity, they are provided to illustrate the best values obtained to date). ^{1}H NMR (CD_2Cl_2, 400.1 MHz, 298 K): δ 7.19 (br s, 2 H, 2 CH of 2 Hpyr), 6.05 (m, 4 H, 4 C*H* of 2 Hpyr), 4.09 (dd, $J_{H\text{-}H}$ = 15.0 Hz, $J_{H\text{-}P}$ = 5.9 Hz, 2 H, 2 C*H* of 2 PCH_2), 3.77 (d, $J_{H\text{-}H}$ = 15.0 Hz, 2 H, 2 C*H* of 2 PCH_2), 1.46 (vt, $J_{H\text{-}P}$ = 7.1 Hz, 18 H, 6 CH_3 of 2 ^{t}Bu), 1.16 (vt, $J_{H\text{-}P}$= 7.1 Hz, 18 H, 6 CH_3 of 2 ^{t}Bu) ppm. ^{13}C{^{1}H} NMR (CD_2Cl_2, 100.6 MHz, 298 K): δ 128.7 (s, *C* of Hpyr), 128.0 (s, *C*H of Hpyr), 110.9 (s, *C*H of Hpyr), 108.0 (s, *C*H of Hpyr), 37.1–36.4 (m, *C* of ^{t}Bu), 30.1 (s, *C*H$_3$ of ^{t}Bu), 29.8 (s, *C*H$_3$ of ^{t}Bu), 24.6 (vt, $J_{C\text{-}P}$ = 12.7 Hz, 2 *C*H$_2$ of 2 PCH_2) ppm.^{31}P{^{1}H} NMR (CD_2Cl_2, 162.1 MHz, 298 K): δ 73.0 (s, sat, $J_{P\text{-}117Sn}$ = 227 Hz, $J_{P\text{-}119Sn}$ = 233 Hz) ppm.

[Pd{κ^3*P*,*Sn*,*P*-Sn(pyrmP^{i}Pr$_2$)$_2$CMe$_2$}] (9): A solution of [Pd(η^3-C_3H_5)(η^5-C_5H_5)] (12 mg, 0.06 mmol) and stannylene **4** (30 mg, 0.05 mmol) in toluene (4 mL) was stirred at room temperature for 16 h. The solvent was removed *in vacuo* and the residue was washed with hexane (4 x 2 mL) to give **9** as a dark green solid (10 mg, 30%). ^{1}H NMR (C_6D_6, 400.1 MHz, 28 K): δ 6.42 (d, $J_{H\text{-}H}$ = 4.0 Hz, 2 H, 2 C*H* of 2 pyr), 6.18 (d, $J_{H\text{-}H}$ = 4.0 Hz, 2 H, 2 C*H* of 2 pyr), 2.99 (d, $J_{H\text{-}H}$ = 16.0 Hz, 2 H, 2 C*H* of 2 CH_2P) 2.79 (dd, $J_{H\text{-}H}$ = 16.0 Hz, $J_{H\text{-}P}$ = 8.0 Hz, 2 H, 2 C*H* of 2 CH_2P), 2.05 (s, 3 H, CH_3 of CMe_2), 1.86 (s, 3 H, CH_3 of CMe_2), 1.70 (m, 2 H, 2 C*H* of 2 $CHMe_2$), 1.48 (m, 2 H, 2 C*H* of 2 $CHMe_2$), 1.01-0.87 (m, 18 H, 6 CH_3 of 6 $CHMe_2$), 0.82 (dd, $J_{H\text{-}H}$ = 8.0 Hz, $J_{H\text{-}P}$ = 4.0 Hz, 6 H, 2 CH_3 of 2 $CHMe_2$) ppm. ^{13}C{^{1}H} NMR (C_6D_6, 100.6 MHz, 298 K): δ 145.9 (s,

C of pyr), 130.5 (s, *C* of pyr), 107.4 (s, *C*H of pyr), 102.9 (s, *C*H of pyr), 39.6 (s, *C*H$_3$ of C*Me*$_2$), 37.8 (s, *C*Me$_2$), 25.8 (s, *C*H$_3$ of C*Me*$_2$), 25.7 (vt, $J_{C\text{-}P}$ = 8.0 Hz, *C*H of CHMe$_2$), 25.2 (vt, $J_{C\text{-}P}$ = 8.0 Hz, *C*H of CHMe$_2$), 24.8 (vt, $J_{C\text{-}P}$ = 10.1 Hz, *C*H$_2$P), 20.8 (s, *C*H$_3$ of CHMe$_2$), 20.3 (s, *C*H$_3$ of CHMe$_2$), 19.4 (s, *C*H$_3$ of CHMe$_2$), 19.0 (s, *C*H$_3$ of CHMe$_2$) ppm. ^{31}P{^{1}H} NMR (C$_6$D$_6$, 162.1 MHz, 298 K): δ 45.1 (s, sat, $J_{P\text{-}119Sn}$ = 41 Hz) ppm.

Computational details

Geometry optimizations were performed without symmetry constraints using the Gaussian09[29] suite of programs at the BP86[30]/def2-SVP[31] level of theory using the D3 dispersion correction suggested by Grimme et al.[32] This level is denoted BP86-D3/def2-SVP. All species discussed in the text were also characterized by frequency calculations and have positive definite Hessian matrices, thus confirming that the computed structures are minima on the potential energy surface. Wiberg Bond Indices (WBIs) and donor-acceptor interactions were computed using the Natural Bond Orbital (NBO6)[33] method. The energies associated with these two-electron interactions have been computed according to the following equation:

$$\Delta E^{(2)}_{\phi\phi^*} = -\,n_\phi \frac{\langle \phi^* | \hat{F} | \phi \rangle^2}{\varepsilon_{\phi^*} - \varepsilon_\phi}$$

where *F* is the DFT equivalent of the Fock operator and ϕ and ϕ^* are two filled and unfilled Natural Bond Orbitals having ε_ϕ and ε_{ϕ^*} energies, respectively; n_ϕ stands for the occupation number of the filled orbital. All QTAIM results described in this work correspond to calculations performed at the BP86-D3/6-31+G(d)/WTBS$_{(\text{transition metals and tin})}$ level on the optimized geometries obtained at the BP86-D3/def2-SVP level. The well-tempered basis sets (WTBS)[34] have been recommended for AIM calculations involving transition metals.[35] The topology of the electron density was conducted using the *AIMAll* program package.[36]

X-Ray diffraction analyses

Crystals of **3**, **4**, **5, 6** and **7**·0.5(C$_6$D$_6$) were analyzed by X-ray diffraction. A selection of crystal, measurement and refinement data is given in Table S1. Diffraction data were collected on an Oxford Diffraction Xcalibur Onyx Nova Geminy with CuKα radiation (for **4**, **6** and **7**·0.5(C$_6$D$_6$) and a Bruker D8 Venture Photon III-14 with MoKα radiation (for **3**·and **5**) single crystal diffractometers. Empirical absorption corrections were applied using the SCALE3 ABSPACK algorithm (as implemented in CrysAlisPro RED[37]) (for **4**, **6** and **7**·0.5(C$_6$D$_6$) and SADABS-2016/2[38] (for **3**·and **5**). A numerical absorption correction based on gaussian integration over a multifaceted crystal model was also applied to **6** and **7**·0.5(C$_6$D$_6$). The structures were solved using SIR-97.[39] Isotropic and full matrix anisotropic least square refinements were carried out using SHELXL.[40] All non-H atoms were refined anisotropically. H atoms were set in calculated positions and were refined riding on their parent atoms. The reflections 0 1 1 and –1 0 1 were left out from the refinement of **3** since their intensities were seriously affected (most likely) by the beam stop, resulting in high S values. Data of **5** were refined as a 2-component inversion twin. Some unusually high residual electron density close to the tin atoms of **5**, which might be caused by (unresolved) twinning, was not assigned. Thermal restrictions were applied to the carbon atoms of one of the SiMe$_3$ moieties of **5** (Si2) due to their tendency to give nonpositive definite ellipsoids. The WINGX program system[41] was used throughout the structure determinations. The molecular plots were made with MERCURY.[42]

Author contributions

The work was conceived and directed by J. A. Cabeza. The experimental work was carried out by C. Laglera-Gándara, R. García-Soriano and R. Toral. I. Fernández performed the DFT calculations. P. García-Álvarez supervised the laboratory experiments. J. A. Cabeza and P. García-Álvarez wrote the manuscript, which was approved by all authors.

Conflicts of interest

There are no conflicts to declare.

Acknowledgements

This work has been supported by research grants obtained from Ministerio de Ciencia e Innovación (PID2019-104652GB-I00, PID2019-106184GB-I00 and RED2018-102387-T). The authors also acknowledge the technical support provided by *Servicios Científico-Técnicos de la Universidad de Oviedo*.

References

1 For selected recent reviews on pincer complexes and their applications, see: (*a*) *Pincer Compounds: Chemistry and Applications*, ed. D. Morales-Morales, Elsevier, Amsterdam, 2018; (*b*) E. Peris, R. H. Crabtree, *Chem. Soc. Rev.,* 2018, **47**, 1959; (*c*) *The Privileged Pincer–Metal Platform: Coordination Chemistry & Applications*, ed. G. van Koten, R. A. Gossage, Springer, Cham, 2016; (*d*) M. Asay and D. Morales-Morales, *Dalton Trans.,* 2015, **44**, 17432; (*e*) C. Gunanathan and D. Milstein, *Chem. Rev.,* 2014, **114**, 12024; (*f*) *Organometallic Pincer Chemistry*, ed. G. van Koten and D. Milstein, Springer, Heidelberg, 2013; (*g*) S. Schneider, J. Meiners and B. Askevold, *Eur. J. Inorg. Chem.,* 2012, 412.

2 For selected reviews on pincer complexes in homogeneous catalysis, see: (*a*) G. Bauer and X. Hu, *Inorg. Chem. Front.,* 2016, **3**, 741; (*b*) H. A. Yonus, W. Su, N. Ahmad, S. Chen and F. Verpoort, *Adv. Synth. Catal.,* 2015, **357**, 283; (*c*) *Pincer and Pincer-Type Complexes: Applications in Organic Synthesis and Catalysis*, ed. K. J. Szabó, O. F. Wendt, Wiley-VCH, Weinheim**,** 2014; (*d*) Q.-H. Dend, R. L. Melen and L. H. Gade, *Acc. Chem. Res.,* 2014, **47,** 3162.

3 See, for example: (*a*) X. Ren, M. Wesolek and P. Braunstein, *Chem. Eur. J.,* 2018, **24**, 14794; (*b*) A. Eizawa, S. Nishimura, K. Arashiba, K. Nakajima and Y. Nishibayashi, *Organometallics,* 2018, **37,** 3086; (*c*) A. Eizawa, K. Arashiba, H. Tanaka, S. Kuriyama, Y. Matsuo, K. Nakajima, K. Yoshizawa and Y. Nishibayashi, *Nat. Commun.,* 2017, **8**, 14874; (*d*) A. G. Nair, R. T. McBurney, M. R. D. Gatus, D. B. Walker, M. Bhadbhade and B. A. Messerle, *J. Organomet. Chem.,* 2017, **845**, 63; (*e*) D. A. Valyaev, J. Willot, L. P. Mangin, D. Zargarian and N. Lugan, *Dalton Trans.,* 2017, **46**, 10193; (*f*) K. Farrel and M. Albrecht**,** in *The Privileged Pincer–Metal Platform: Coordination Chemistry & Applications*, ed. G. van Koten, R. A. Gossage, Springer, Cham, 2016, p. 45.

4 See, for example: (*a*) Z. Benedek and T. Szilvási, *Organometallics,* 2017, **36**, 1591; (*b*) A. Rosas-Sánchez, I. Alvarado-Beltrán, A.

Baceiredo, N. Saffon-Merceron, S. Massou, V. Ranchadell and T. Kato, *Angew. Chem. Int. Ed.,* 2017, **56,** 10549; (*c*) Y.-P. Zhou, S. Raoufmoghaddam, T. Szilvási and M. Driess, *Angew. Chem. Int. Ed.,* 2016, **55**, 12868; (*d*) T. Troadec, A. Prades, R. Rodriguez, R. Mirgalet, A. Baceiredo, N. Saffon-Merceron, V. Branchadell and T. Kato, *Inorg. Chem.,* 2016, **55**, 8234; (*e*) J. A. Cabeza, P. García-Álvarez, R. Gobetto, L. González-Álvarez, C. Nervi, E. Pérez-Carreño and D. Polo, *Organometallics,* 2016, **35,** 1761; (*f*) Z. Benedek and T. Szilvási, *RSC Adv.,* 2015, **5**, 5077; (*g*) L. Álvarez-Rodríguez, J. A. Cabeza, P. García-Álvarez and D. Polo, *Coord. Chem. Rev.,* 2015, **300**, 1; (*h*) G. Tan, S. Enthaler, S. Inoue, B. Blom and M. Driess, *Angew. Chem. Int. Ed.,* 2015, **54**, 2214; (*i*) L. Álvarez-Rodríguez, J. A. Cabeza, P. García-Álvarez, E. Pérez-Carreño and D. Polo, *Inorg. Chem.,* 2015, **54**, 2983; (*j*) J. A. Cabeza, P. García-Álvarez, E. Pérez-Carreño and D. Polo, *Chem. Eur. J.,* 2014, **20**, 8654.

5 For a recent review on silylene transition-metal complexes in catalysis, see: Y.-P. Zhou and M. Driess, *Angew. Chem. Int. Ed.,* 2019, **58**, 3715.

6 See, for example: (*a*) Y.-P. Zhou, Z. Mo, M.-P. Luecke and M. Driess, *Chem. Eur. J.,* 2018, **24**, 4780; (*b*) J. A. Cabeza, P. García-Álvarez and L. González-Álvarez, *Chem. Commun.,* 2017, **53**, 10275; (*c*) T. Iimura, N. Akasaka, T. Kosai and T. Iwamoto, *Dalton Trans.,* 2017, **46**, 8868; (*d*) H. Ren, Y.-P. Zhou, Y. Bai, C. Cui and M. Driess, *Chem. Eur. J.,* 2017, **23**, 566; (*e*) T. Iimura, N. Akasaka and T. Iwamoto, *Organometallics,* 2016, **35**, 4071; (*f*) L. Álvarez-Rodríguez, J. A. Cabeza, J. M Fernández-Colinas, P. García-Álvarez and D. Polo, *Organometallics,* 2016, **35**, 2516; (*g*) Y.-P. Zhou, S. Raoufmoghaddam, T. Szilvási and M. Driess, *Angew. Chem. Int. Ed.,* 2016, **55**, 12868; (*h*) T. T. Metsänen, D. Gallego, T. Szilvási, M. Driess and M. Oestreich, *Chem. Sci.,* 2015, **6**, 7143; *(i*) D. Gallego, S. Inoue, B. Blom and M. Driess, *Organometallics,* 2014, **33**, 6885; (*j*) D. Gallego, A. Brück, E. Irran, F. Meier, F. Kaupp and M. Driess, *J. Am. Chem. Soc.,* 2013, **135**, 15617; (*k*) A. Brück, D. Gallego, W. Wang, E. Irran, M. Driess and J. F. Hartwig, *Angew. Chem. Int. Ed.,* 2012, **51**, 11478; (*l*) S. Li, Y. Wang, W. Yang, K. Li, H. Sun, X. Li, O. Fuhr and D. Fenske, *Organometallics,* 2020, **39**, 757; (*m*) N. Parvin, B. Mishra, M. Neralkar, J. Hossain, P. Parameswaran, S. Hotha and S. Kahn, *Chem. Commun.,* 2020, **56**, 7625; (*n*) R. Arevalo, T. P. Pabst and P. J. Chirik, *Organometallics,* 2020, **39**, 2763; (*o*) J. A. Cabeza and P. García-Álvarez, *Eur. J. Inorg. Chem.,* 2021, 3315.

7 W. Wang, S. Inoue, E. Irran and M. Driess, *Angew. Chem. Int. Ed.,* 2012, **51**, 3691.

8 (*a*) M. T. Whited, J. Zhang, S. Ma, B.D. Nguyen and D. E. Janzen, *Dalton Trans,.* 2017, **46**, 14757; (*b*) J. C. DeMott, W. X. Gu, B. J. McCulloch, D. E. Herbert, M. D. Goshert, J. R. Walensky, J. Zhou and O. V. Ozerov, *Organometallics,* 2015, **34**, 3930; (*c*) H. Handwerker, M. Paul, J. Blumel and C. Zybill, *Angew. Chem. Int. Ed.,* 1993, **32**, 1313.

9 (*a*) Y. Cabon, H. Kleijn, M. A. Siegler, A. L. Spek, R. J. M. Gebbink and B.-J. Deelman, *Dalton Trans*., 2010, **39**, 2423; *(b*) S. Warsink, E. J. Derrah, C. A. Boon, Y. Cabon, J. J. M. de Pater, M. Lutz, R. J. M. Gebbink and B.-J. Deelman, *Chem. Eur. J*., 2015, **21**, 1765.

10 L. Álvarez-Rodríguez, J. Brugos, J. A. Cabeza, P. García-Álvarez, E. Pérez-Carreño and D. Polo, *Chem. Commun.,* 2017, **53**, 893.

11 S. Bestgen, N. H. Rees and J. M. Goicoechea, *Organometallics,* 2018, **37**, 4147.

12 J. A. Cabeza, I. Fernández, J. M. Fernández-Colinas, P. García-Álvarez and C. J. Laglera-Gándara, *Chem. Eur. J.,* 2019, **25**, 12423.

13 J. A. Cabeza, I. Fernández, P. García-Álvarez and C. J. Laglera-Gándara, *Dalton Trans.,* 2019, **48**, 13273.

14 T. Watanabe, Y. Kasai and H. Tobita, *Chem. Eur. J.,* 2019, **25**, 13491.

15 S. Bestgen, M. Mehta, T. C. Johnstone, P. W. Roesky and J. M. Goicoechea, *Chem. Eur. J.,* 2020, **26**, 9024.

16 J. Brugos, J. A. Cabeza, P. García-Álvarez and E. Pérez-Carreño, D. Polo, *Dalton Trans.,* 2018, **47**, 4534.

17 J. A. Cabeza, P. García-Álvarez and C. J. Laglera-Gándara, *Eur. J. Inorg. Chem.,* 2020, 784.

18 (*a*) L. Álvarez-Rodríguez, J. Brugos, J. A. Cabeza, P. García-Álvarez and E. Pérez-Carreño, *Chem. Eur. J.,* 2017, **23**, 15107; (*b*) J. Brugos, J. A. Cabeza, P. García-Álvarez and E. Pérez-Carreño, *Organometallics,* 2018, **37**, 1507.

19 (*a*) J. A. Cabeza, P. García-Álvarez, C. J. Laglera-Gándara and E. Pérez-Carreño, *Chem. Commun*., 2020, **56**, 14095; (*b*) A. Arauzo, J. A. Cabeza, I. Fernández, P. García-Álvarez, I. García-Rubio and C. J. Laglera-Gándara, *Chem. Eur. J.,* 2021, **27**, 4985; (*c*) J. A. Cabeza, P. García-Álvarez, C. J. Laglera-Gándara, E. Pérez-Carreño and *Eur. J. Inorg. Chem.,* 2021, 1897.

20 J. D. Parish, M. W. Snook, A. J. Johnson and G. Kociok-Kohn, *Dalton Trans.,* 2018, **47**, 7721.

21 (*a*) C. R. Wade, T.-P. Lin, R. C. Nelson, E. A. Mader, J. T. Miller and F. P. Gabbaï, *J. Am. Chem. Soc.,* 2011, **133,** 8948; (*b*) H. Yang and F. P. Gabbaï, *J. Am. Chem. Soc,*. 2015, **137**, 13425; (*c*) S. Sen, I.-S. Ke and F. P. Gabbaï, *Inorg. Chem*., 2016, **55**, 9162; (*d*) S. Sen, I.-S. Ke and F. P. Gabbaï, *Organometallics,* 2017, **36**, 4224; (*e*) F. Inagaki, C. Matsumoto, Y. Okada, N. Maruyama and C. Mukai, *Angew. Chem. Int. Ed.,* 2015, **54**, 818; (*f*) G. Kleinhans, M. M. Hansmann, G. Guisado-Barrios, D. C. Liles, G. Bertrand and D. I. Bezuidenhout, *J. Am Chem. Soc.,* 2016, **138**, 15873; (*g*) J.-Y. Hu, J. Zhang, G.-X. Wang, H.-L-. Sun and J.-L. Zhang, *Inorg. Chem.,* 2016, **55**, 2274; (*h*) G. Kleinhans, A. K.-W. Chan, M.-Y. Leung, D. C. Liles, M. A. Fernandes, V. W.-W. Yam, I. Fernández and D. I. Bezuidenhout, *Chem. Eur. J.,* 2020, **26**, 6993.

22 See, for example: (*a*) D. M. Norton, E. A. Mitchell, N. R. Botros, P. G. Jessop and M. C. Baird, *J. Org. Chem.,* 2009, **74**, 6674; (*b*) P. Steinhoff, M. Paul, J. P. Schroers and M. E. Taucher, *Dalton Trans.,* 2019, **48**, 1017.

23 See, for example: (*a*) P. Steinhoff and M. E. Tauchert, *Beilstein J. Org. Chem.,* 2016, **12**, 1573; (*b*) S. Arifhodzic-Radojevic, A. D. Burrows, N. Choi, M. McPartlin, D. M. P. Mingos, S. V. Tarlton and R. Vilar, *J. Chem. Soc., Dalton Trans.,* 1999, 3981; (*c*) J. Bauer, H. Braunschweig, A. Damme, K. Gruss and K. Radacki, *Chem. Commun.,* 2011, **47**, 12783.

24 See, for example: (*a*) A. Amgoune and D. Bourissou, *Chem. Commun.,* 2011, **47**, 859; (*b*) G. Bouhadir and D. Bourissou, in *The Chemical Bond III. Structure and Bonding*, vol. 171, ed. D. M. P. Mingos, Springer, Cham, 2016, p. 141, DOI: 10.1007/430_2015_201; (*c*) R. Murakami and F. Inagaki, *Tetrahedron Lett.,* **2019**, **60**, 151231; (*d*) D. You and F. P. Gabbaï, *Trends in Chem.,* 2019, **1**, 485, DOI: 10.1016/j.trechm.2019.03.011.

25 K. M. Krebs, S. Freitag, H. Schubert, B. Gerke, R. Pöttgen and L. Wesemann, *Chem. Eur. J.,* 2015, **21**, 4628.

26 R. Usón, A. Laguna, M. Laguna, D. A. Briggs, H. H. Murray and J. Fackler, *Inorg. Synth*., 1989, **26**, 85.

27 Y. Tatsuno, T. Yoshida and S. Otsuka, *Inorg. Synth.,* 1979**, 19**, 220.

28 M. J. S. Gynane, D. H. Harris, M. F. Lappert, P. P. Power, P. Riviere and M. Riviere-Baudet, *J. Chem. Soc., Dalton Trans.,* 1977, 2004.

29 *Gaussian 09*, revision D.01: M. J. Frisch, G. W. Trucks, H. B. Schlegel, G. E. Scuseria, M. A. Robb, J. R. Cheeseman, G. Scalmani, V. Barone, B. Mennucci, G. A. Petersson, H. Nakatsuji, M. Caricato, X. Li, H. P. Hratchian, A. F. Izmaylov, J. Bloino, G. Zheng, J. L. Sonnenberg, M. Hada, M. Ehara, K. Toyota, R. Fukuda, J. Hasegawa, M. Ishida, T. Nakajima, Y. Honda, O. Kitao, H. Nakai, T. Vreven, J. A. Montgomery, Jr., J. E. Peralta, F. Ogliaro, M. Bearpark, J. J. Heyd, E. Brothers, K. N. Kudin, V. N. Staroverov, R. Kobayashi, J. Normand, K. Raghavachari, A. Rendell, J. C. Burant, S. S. Iyengar, J. Tomasi, M. Cossi, N. Rega, N. J. Millam, M. Klene, J. E. Knox, J. B. Cross, V. Bakken, C. Adamo, J. Jaramillo, R. Gomperts, R. E. Stratmann, O. Yazyev, A. J. Austin, R. Cammi, C. Pomelli, J. W. Ochterski, R. L. Martin, K. Morokuma, V. G. Zakrzewski, G. A. Voth, P. Salvador, J. J. Dannenberg, S. Dapprich, A. D. Daniels, Ö. Farkas, J. B. Foresman, J. V. Ortiz, J. Cioslowski and D. J. Fox, Gaussian, Inc., Wallingford, CT, 2009.

30 (*a*) A. D. Becke, *J. Phys. Chem. A* 1988, **38**, 3098; (*b*) J. P. Perdew, *Phys. Rev. B,* 1986, **33**, 8822.

31 F. Weigend and R. Ahlrichs, *Phys. Chem. Chem. Phys*., 2005, **7**, 3297.

32 S. Grimme, J. Antony, S. Ehrlich and H. Krieg, *J. Chem. Phys*., 2010, **132**, 154104.

33 (*a*) J. P. Foster and F. Weinhold, *J. Am. Chem. Soc*., 1980, **102**, 7211; (*b*) A. E. Reed and F. Weinhold, *J. Chem. Phys*., 1985, **83**, 1736; (*c*) A. E. Reed, R. B. Weinstock and F. Weinhold, *J. Chem. Phys*., 1985, **83**,

735; (*d*) A. E. Reed and L. A. Curtiss, F. Weinhold, *Chem. Rev*., 1988, **88**, 899.
34 (*a*) S. Huzinaga and B. Miguel, *Chem. Phys. Lett*., 1990, **175**, 289; (*b*) S. Huzinaga and M. Klobukowski, *Chem. Phys. Lett*., 1993, **212**, 260.
35 J. A. Cabeza, J. F. van der Maelen and S. García-Granda, *Organometallics*, 2009, **28,** 3666 and references therein.
36 *AIMAll*, version 19.02.13: T. A. Keith, http://tkgristmill.com.
37 *CrysAlisPro RED*, version 1.171.37.35: Oxford Diffraction Ltd., Oxford, UK, 2014.
38 *SADABS-2016/2*: L. Krause, R. Herbst-Irmer, G. M. Sheldrick and D. Stalke, *J. Appl. Crystallogr*., 2015, **48**, 3.
39 *SIR-97*: A. Altomare, M. C. Burla, M. Camalli, G. L. Cascarano, C. Giacovazzo, A. Guagliardi, A. G. C. Moliterni, G. Polidori and R. Spagna, *J. Appl. Crystallogr*., 1999, **32**, 115.
40 *SHELXL-2014*: G. M. Sheldrick, *Acta Cryst*., 2008, **A64**, 112.
41 *WINGX*, version 2013.3: J. Farrugia, *J. Appl. Crystallogr*., 2012, **45**, 849.
42 *MERCURY*, version 2020.1 (build 280191): Cambridge Crystallographic Data Centre, Cambridge, UK, 2018.

Dalton Transactions

ARTICLE

Figure and Text for the Table of Contents

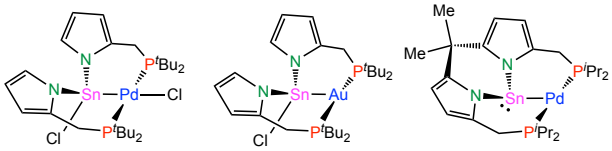

Metal complexes containing PSnP pincer stannyl and stannylene ligands have been prepared form new pyrrole- and dipyrromethane-based PSnP stannylenes.